Eur. Phys. J. D **18**, 251–258 (2002)
DOI: 10.1140/epjd/e20020030

THE EUROPEAN PHYSICAL JOURNAL D
EDP Sciences

Comprehensive experimental test of quantum erasure

A. Trifonov[1,2,a], G. Björk[1], J. Söderholm[1], and T. Tsegaye[1]

[1] Department of Microelectronics and Information Technology, Royal Institute of Technology (KTH), Electrum 229, 16440 Kista, Sweden
[2] Ioffe Physical Technical Institute, 26 Polytekhnicheskaya, 194021 St. Petersburg, Russia

Received 15 July 2001 and Received in final form 30 November 2001

Abstract. In an interferometer, path information and interference visibility are incompatible quantities. Complete determination of the path will exclude any possibility of interference, rendering zero visibility. However, it is, under certain conditions, possible to trade the path information for improved (conditioned) visibility. This procedure is called quantum erasure. We have performed such experiments with polarization-entangled photon pairs. Using a partial polarizer, we could vary the degree of entanglement between the object and the probe. We could also vary the interferometer splitting ratio and thereby vary the *a priori* path predictability. This allowed us to test quantum erasure under a number of different experimental conditions. All experiments were in good agreement with theory.

PACS. 03.65.Ta Foundations of quantum mechanics; measurement theory – 42.50.-p Quantum optics

1 Introduction

A fundamental difference between classical physics and quantum mechanics is that the latter, being a linear dynamical theory, allows superpositions. The superposition principle, in turn, leads to the concept of complementarity, the fact that any quantum system has at least two properties that cannot simultaneously be known with certainty. Complementarity has been discussed intensively since the early development of quantum mechanics [1,2]. Recently, some new qualitative statements about complementarity have been proposed [3–12], and subsequently the question has been raised whether there exist any relations between these new expressions and the Schrödinger-Robertson and the Arthurs-Kelly uncertainty principles [8,9,11,13,14]. In addition, the fundamental physical mechanism that enforces complementarity has been debated [14–17].

When deriving his uncertainty principle, Heisenberg erroneously attributed the uncertainty to the back-action on the measured object from the measurement apparatus. Later work has clarified that Heisenberg's uncertainty relation only makes a statement about the preparation of a quantum mechanical state. If one wants to qualitatively record the back-action on the state due to a measurement of some observable $\hat{A}$, one also has to measure the conjugate observable to $\hat{A}$ on the "same" state. (Unless the state is an eigenstate of $\hat{A}$, the state will change as a result of the $\hat{A}$-measurement. Therefore, we have put the word "same" within quotation marks.) This is often called a simultaneous measurement, *i.e.*, on every member of an ensemble two incompatible measurements are made. Examining the uncertainty product of the two simultaneous measurements, one arrives at quantitatively, or even qualitatively, different uncertainty principles from that of Heisenberg [13,18–23]. What is surprising is that the back-action, or at least the measured uncertainty due to the back-action, is not solely a property of the object and the object-probe interaction, but depends also on how the probe is measured and how the obtained information is used. Under certain circumstances, the apparent indeterminism of the object due to the measurement back-action can be undone by the action of a *local* operation on the probe. This procedure is called quantum erasure [24] and is a manifestation of the nonlocality of quantum mechanics. Various implementations of such experiments, and their connection to complementarity have been discussed in some recent papers [6,12,13,25]. Several experiments have also been performed [26–34]. What distinguishes our experiment from the previous ones is that we have been able to vary both the degree of object and probe entanglement and, independently, the *a priori* path information. This leads to a more complex situation than previously reported.

In order to discuss quantum erasure in greater detail, we will start by making a few definitions. Quantum mechanics only makes predictions about states. It does not say anything about paths, modes or objects. All these words are classical concepts, but are nonetheless useful in discussions about quantum erasure. Usually quantum erasure is discussed in the context of an object passing through one of two slits in Young's double-slit experiment, or taking one of two paths in an interferometer. Strictly speaking, the two paths are described by two orthogonal modes. The object's possible paths are then defined by two state vectors $|O_+\rangle$ and $|O_-\rangle$. In general, this description is insufficient to describe all possible outcomes of an

[a] e-mail: alexei@ele.kth.se

experiment. In this case, one can define two sets of states $\{|O_{+,i}\rangle\}$ and $\{|O_{-,i}\rangle\}$, where all states are mutually orthonormal. This is, *e.g.*, the case in a recent experiment by Schwindt *et al.* [35], where the paths were defined in terms of two spatial modes, and in each of the paths the object could be either in a vertically or horizontally polarized state (or in a superposition or mixture of the two polarization states). However, to describe our experiment, we only need a two-dimensional object Hilbert space $\mathcal{H}_{\mathrm{O}}$, which was the case treated in references [11,12]. Note that it is not necessary to take the concept of "path" literally when we consider complementarity. In our experiment, the two modes corresponding to the "paths" are actually two orthogonal linear polarization modes, or equivalently, two orthogonal polarization states in the same spatial mode.

The only *a priori* information we have about the path taken by the object is the corresponding probabilities w_+ and $w_- = 1 - w_+$, which are given by the prepared state of the object. Adopting the maximum likelihood estimation strategy, we should, for each and every event, guess that the object took the most likely "path". The strategy will maximize the likelihood L of guessing the "path" correctly. The likelihood will be $L = \mathrm{Max}\{w_+, w_-\}$, which means that $1/2 \leq L \leq 1$. The likelihood can be renormalized to yield the statistical predictability P, defined as [10,11]

$$P = 2L - 1. \tag{1}$$

It is clear that $0 \leq P \leq 1$, where $P = 0$ corresponds to a random guess of which "path" the object took, and $P = 1$ corresponds to absolute certainty about the "path".

One can also compute the visibility when the two "path" probability amplitudes interfere. The visibility V_0, too, is a statistical measure, which requires an ensemble of identically prepared systems to be estimated. Since we are dealing with single quanta, we can express the visibility in the probability for the object to exit one of the two interferometer ports

$$V_0 = \frac{p_{\max} - p_{\min}}{p_{\max} + p_{\min}}, \tag{2}$$

where $p_{\max}$ ($p_{\min}$) is the maximum (minimum) probability of detection of the object when the "paths" interfere.

It has been shown [4] that P and V_0 for an object whose "path" is determined by one of two orthonormal states, satisfies the inequality

$$P^2 + {V_0}^2 \leq 1, \tag{3}$$

where the upper bound is saturated for any pure state. Note that if one wants to verify the inequality (3) experimentally, one needs two ensembles of identical states. On the first ensemble one makes a "path" measurement, and on the second one makes a visibility measurement. Hence, on any individual member of the ensemble, only one (sharp) measurement is performed.

2 Probing the "path"

In order to retrieve more information about the "path" of the object than what is given by the *a priori* "path" probabilities w_+ and w_-, it is possible to use an ancillary probe system. This is achieved by an interaction between the object and probe, which entangles their degrees of freedom. In this way, we can simultaneously get "path" information (from the probe ancilla) and visibility information (from the object). In order for the probe to carry any information about the path taken by the object, the probe's state must be allowed to vary in a Hilbert space $\mathcal{H}_{\mathrm{M}}$ of at least a dimension two, as a result of the interaction. Hence, in the simplest case, the state of the total system after the interaction belongs to a 2×2-dimensional composite Hilbert space $\mathcal{H}_{\mathrm{O}} \otimes \mathcal{H}_{\mathrm{M}}$. The first space describes the object, whose "path" and visibility we wish to measure, and the second describes the probe, that will help us to get information about the object's "path". We assume that the interaction between the object and probe leaves the probabilities w_+ and w_- invariant. This is not the most general entangling interaction possible, but defines the subset of entangling interactions of the quantum nondemolition (QND) kind [12].

A few different experimental situations can be distinguished:

1. the state after the interaction can be factorized in the two Hilbert spaces $\mathcal{H}_{\mathrm{O}}$ and $\mathcal{H}_{\mathrm{M}}$. Then both systems can be treated independently. The state of the probe carries no information about the object and vice versa. This is a trivial and not particularly interesting situation;
2. the state is a perfectly entangled state so that the probe contains full "path" information of the object. Thus, our ability to predict which "path" the object took is perfect, while the visibility is zero. To retrieve the original visibility, it is necessary to give up the "path" information. To this end, the probe must be measured in such a way that the information encoded in the state of the probe is not revealed by the measurement, *i.e.*, the probe measurement must correspond to a complementary observable to the one that discloses the "path";
3. the state is partially entangled. This is an intermediate case between the previous two. Only partial information about the "path" of the object can be extracted from the probe. That still leaves room for a non-zero visibility. This intermediate case is examined carefully in the present paper.

The most general scheme of the measuring procedure is shown in Figure 1. The object can take one of two "paths" and the probe is used to determine which "path" the object took. Before the interaction (plane A), the object and the probe are independent, and the state is represented by a product of the corresponding density operators

$$\hat{\rho} = \hat{\rho}_{\mathrm{O}} \otimes \hat{\rho}_{\mathrm{M}}, \tag{4}$$

where $\hat{\rho}_{\mathrm{O}} = |\Psi_{\mathrm{O}}\rangle \langle\Psi_{\mathrm{O}}|$ and

$$|\Psi_{\mathrm{O}}\rangle = \sqrt{w_+}\,|O_+\rangle + \mathrm{e}^{\mathrm{i}\phi}\sqrt{w_-}\,|O_-\rangle\,.$$

This is not the most general $\hat{\rho}_{\mathrm{O}}$, since it represents a pure state. However, only pure states saturate equation (3), so we will restrict ourselves to this case.

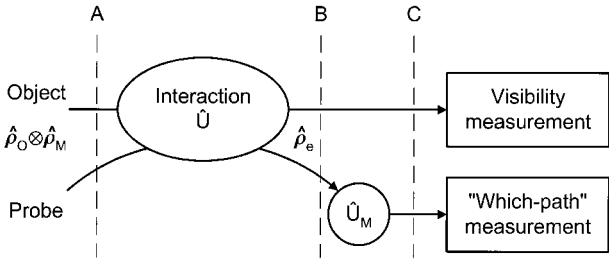

Fig. 1. Schematic setup for a QND-type measurement of the complementary "path" and visibility observables. $\hat{U}_{\rm M}$ symbolizes a local unitary transformation of the probe, applied before the probe state is irrevocably collapsed by the "which-path" meter.

The role of the interaction is to entangle the object and the probe. We assume that the interaction affects only the probe's degrees of freedom, and that it is described by a unitary transformation $\hat{U}$ such that

$$\begin{aligned}\hat{U}\,|O_+\rangle\,|M\rangle &= |O_+\rangle\,|m_+\rangle\,,\\ \hat{U}\,|O_-\rangle\,|M\rangle &= |O_-\rangle\,|m_-\rangle\,,\end{aligned} \tag{5}$$

where $|M\rangle$ is the initial probe state. The state after the interaction (plane B) then becomes

$$|\Psi_{\rm e}\rangle = \sqrt{w_+}\,|O_+\rangle\,|m_+\rangle + {\rm e}^{{\rm i}\phi}\sqrt{w_-}\,|O_-\rangle\,|m_-\rangle\,\cdot \tag{6}$$

The corresponding density operator is denoted $\hat{\rho}_{\rm e}$. If $\langle m_+|m_-\rangle = 0$, we have perfect entanglement and the "path" taken by the object can be extracted perfectly from a measurement of the probe. It is convenient to introduce

$$c = |\langle m_+|m_-\rangle|\,, \tag{7}$$

which is a measure of the entanglement, since the object states $|O_+\rangle$ and $|O_-\rangle$ are fixed. If there is no entanglement then $|m_+\rangle = |m_-\rangle$, which implies $c = 1$.

From an experimental point of view, it is more convenient to deal with an orthogonal probe basis $|M_+\rangle$ and $|M_-\rangle$. It is always possible to choose, for simplicity, $\langle m_+|M_-\rangle = 0$. In this new basis, we have

$$\begin{aligned}|\Psi_{\rm e}\rangle = \sqrt{w_+}\,|O_+\rangle\,|M_+\rangle + {\rm e}^{{\rm i}\phi}c\sqrt{w_-}\,|O_-\rangle\,|M_+\rangle\\ +{\rm e}^{{\rm i}\phi}\sqrt{w_-(1-c^2)}\,|O_-\rangle\,|M_-\rangle\,\cdot\end{aligned} \tag{8}$$

One of the simplest experimental realizations of this state is a superposition of two single-photon two-mode states. Unfortunately, the strength of the state-of-the-art nonlinear interaction at single-photon level is too weak to produce the state (8) from (4) by interaction of the object and probe photons. Therefore, it is tempting to try to generate the state (8) by using spontaneous parametric down-conversion (SPDC) in which a pump photon is split into a pair of photons. In Section 4, we will show that under certain conditions the state (8) can be produced in this way. But first, let us introduce the quantities of interest in our treatment of "path" information and visibility.

3 Distinguishability and visibility

The complementary nature of the object before the interaction with the probe is fully described by P and V_0. The predictability can be computed from $\hat{\rho}_{\rm e}$ as

$$\begin{aligned}P &= |w_+ - w_-|\\ &= |\langle O_+|\,{\rm Tr}_{\rm M}\{\hat{\rho}_{\rm e}\}\,|O_+\rangle - \langle O_-|\,{\rm Tr}_{\rm M}\{\hat{\rho}_{\rm e}\}\,|O_-\rangle|\,,\end{aligned} \tag{9}$$

where the trace is taken over the probe Hilbert space. By our choice of interaction (QND-type of entanglement), the predictability remains invariant, but the post-interaction visibility will, in general, be smaller than the pre-interaction visibility. The visibility can be computed from

$$V = 2\,|\langle O_+|\,{\rm Tr}_{\rm M}\{\hat{\rho}_{\rm e}\}\,|O_-\rangle|\,. \tag{10}$$

These expressions are consistent with equations (1, 2). Since the visibility is not a conserved quantity, we have denoted the pre-interaction visibility V_0. In general $V \leq V_0$, which can be attributed to random relative-phase shifts associated with the interaction process [17].

The appropriate measure of the post-interaction "path" information is the distinguishability, which is given by

$$D = {\rm Tr}_{\rm M}\left\{\|\langle O_+|\,\hat{\rho}_{\rm e}\,|O_+\rangle - \langle O_-|\,\hat{\rho}_{\rm e}\,|O_-\rangle\|\right\}, \tag{11}$$

where $\|\hat{a}\|$ denotes the trace-class norm of $\hat{a}$ (see for example [36]). Choosing the entanglement interaction in the way we did ensures that $P \leq D$. As it was shown by Englert [11], complementarity leads to the inequality

$$D^2 + V^2 \leq 1. \tag{12}$$

This expression has a clear physical explanation: it is possible to get more information about the "path" (D) only on the expense of the conjugate observable, which is the relative phase and is quantified by V for the present case [13,17]. It means that D contains both the *a priori* "path" information and the additional information encoded in the entanglement between the object and the probe. It should be noted that the distinguishability denotes the maximum information about the "path" that can be extracted from the probe by a measuring apparatus. All this information can be gained, *e.g.*, by using an optimal probe state projection onto photodetectors. This can be accomplished by adjusting the unitary evolution $\hat{U}_{\rm M}$ preceding the photodetectors (see Fig. 1).

For an arbitrary, in general non-optimal, probe measurement basis, the quantitative measure of obtained "path" information is the so-called measured distinguishability [12] (the same quantity is called "knowledge" by Englert [35]). It can mathematically be expressed as

$$\begin{aligned}D_{\rm m} = \left|\langle M_+|\,\hat{U}_{\rm M}\left(\langle O_+|\,\hat{\rho}_{\rm e}\,|O_+\rangle - \langle O_-|\,\hat{\rho}_{\rm e}\,|O_-\rangle\right)\hat{U}_{\rm M}^{\dagger}\,|M_+\rangle\right|\\ +\left|\langle M_-|\,\hat{U}_{\rm M}\left(\langle O_+|\,\hat{\rho}_{\rm e}\,|O_+\rangle - \langle O_-|\,\hat{\rho}_{\rm e}\,|O_-\rangle\right)\hat{U}_{\rm M}^{\dagger}\,|M_-\rangle\right|\cdot\end{aligned} \tag{13}$$

Table 1. "Which-path" and visibility quantities, and their mutual relations.

	Quantities determined by the reduced object state $\hat{\rho}'_{\rm O} = {\rm Tr}_{\rm M}\{\hat{\rho}_{\rm e}\}$		Quantities determined by the composite state $\hat{\rho}_{\rm e}$ and the choice of probe basis		Quantities determined by the composite state $\hat{\rho}$ (or $\hat{\rho}_{\rm e}$)
"Which path"	P	$\leq$	$D_{\rm m}$	$\leq$	D
Visibility	$V = \sqrt{1-D^2}$	$\leq$	$V_{\rm c}$	$\leq$	$V_0 = \sqrt{1-P^2}$

Similarly, the associated visibility, conditioned on the outcome of the probe measurement, can be expressed as

$$V_{\rm c} = 2\left|\langle M_+|\,\hat{U}_{\rm M}\,\langle O_+|\,\hat{\rho}_{\rm e}\,|O_-\rangle\,\hat{U}^{\dagger}_{\rm M}\,|M_+\rangle\right| + 2\left|\langle M_-|\,\hat{U}_{\rm M}\,\langle O_+|\,\hat{\rho}_{\rm e}\,|O_-\rangle\,\hat{U}^{\dagger}_{\rm M}\,|M_-\rangle\right|. \quad (14)$$

To interpret the equation above in terms of a concrete measurement procedure, the visibility data should be sorted in two sets depending on the outcome of the (binary) probe measurement. The conditioned visibility is then the probability weighted average of the two obtained visibilities. It can be seen directly from the form of equations (10, 14) that $V \leq V_{\rm c} \leq V_0$. The relations between all quantities for a pure state are summarized in Table 1 and by the inequalities (3, 12).

As was shown in reference [13], there exists a mutual symmetry between P and V_0. The symmetry implies that the visibility can be treated as predictability, if the observables corresponding to the "path" measurement and the visibility measurement are exchanged. However, entanglement of the kind (5) breaks this symmetry: with the chosen entanglement it is only feasible to get more information about the "path" $D \geq P$ (see Tab. 1) at the expense of the visibility. In the "best" case (optimal quantum erasure) it is possible to restore the initial visibility.

4 Experimental test of complementarity

A pair of polarization-entangled photons was used to produce the state (8). Unfortunately, state-of-the-art technology does not allow us to perform the entangling step transforming (4) into (6) using a pair of photons. Therefore, we start directly with the state (6) without introducing unentangled object and probe states first. This is not such a serious flaw as it may appear. If we had started with unentangled states we would have had to make sure that the state $|\Psi_{\rm e}\rangle$ was indeed produced, by measuring, *e.g.*, w_+, c, and ϕ. Hence, there is actually little point in using a two-step procedure to arrive at $|\Psi_{\rm e}\rangle$, since the parameters w_+ and ϕ (uniquely defining $|\Psi_{\rm O}\rangle$) can, and must, be measured from $|\Psi_{\rm e}\rangle$ anyhow.

The basic experimental setup is shown in Figure 2. It is similar to that described in [37], but we have used a pulsed pump source (a Ti:sapphire laser emitting at 780 nm incorporating frequency doubling to 390 nm). The length of the pump pulse was chosen to be 1 ps, which is long enough to minimize the group-velocity dispersion. The use of a pulsed source reduced substantially the random coincidence counts between signal photons and dark counts, and between coincident dark counts. Thus, no dark-count corrections were made in any of the data presented in this paper. A beta-barium borate (BBO) crystal with type-I phase matching was used for frequency doubling and a type-II BBO crystal was used for SPDC. Special care was taken to compensate for the residual BBO group-velocity mismatch. In our experiments, we used EG&G single-photon detectors with a quantum efficiency of about 60%. Identical 10-nm bandpass filters were placed in front of each of the detectors to select degenerate photon pairs. Furthermore, two polarizers were used to select linearly polarized photons. Polarization rotation was accomplished by two $\lambda/2$-plates placed in front of the polarizers. In this way, we were able to make coincidence measurements of any combination of linear polarizations in the object and probe modes. A 94% fringe visibility in coincidence measurement was observed when one $\lambda/2$-plate was fixed at 22.5° with respect to the BBO principal axes (horizontal-vertical) and the other $\lambda/2$-plate was rotated.

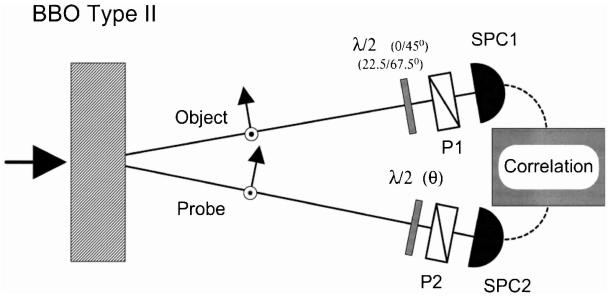

Fig. 2. Experimental setup for testing complementarity by the means of photon polarization measurements on maximally entangled photon pairs. The labels SPC, P, and $\lambda/2$ signify single-photon counters, polarizers, and half-wave plates, respectively.

4.1 A maximally entangled state

Let us start with the state that was produced in the experiment by the BBO crystal (followed by state postselection to eliminate the predominant $|0,0\rangle$-state)

$$|\Psi^-\rangle = \frac{1}{\sqrt{2}}\left(|\uparrow,\rightarrow\rangle - |\rightarrow,\uparrow\rangle\right), \quad (15)$$

where $\uparrow$ and $\rightarrow$ indicate a vertically and a horizontally polarized photon, respectively. Using the notation we have

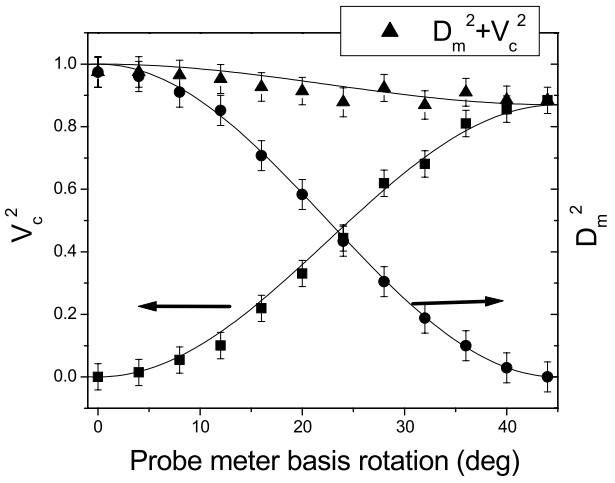

Fig. 3. Results for measured distinguishability and conditioned visibility versus probe meter basis rotation. Lines represent the theoretical values as the non-perfect mode overlap is taken into account (see text for details).

introduced in the previous sections, we write

$$\left|\Psi^-\right\rangle = \frac{1}{\sqrt{2}}\left(|O_+, M_+\rangle - |O_-, M_-\rangle\right)\cdot \qquad (16)$$

This state corresponds to the second of the experimental situations listed in Section 2. For such a state $P = 0$, $D = 1$, and $V = 0$. The measured distinguishability $D_{\mathrm{m}}(\theta)$ and the conditioned visibility $V_{\mathrm{c}}(\theta)$ were measured for different choices of probe basis. As described above, the probe basis was chosen by rotating the $\lambda/2$-plate in front of the probe detector. This corresponds to different $\hat{U}_{\mathrm{M}}$ according to

$$\begin{pmatrix} |M_+(\theta)\rangle \\ |M_-(\theta)\rangle \end{pmatrix} = \begin{pmatrix} \hat{U}^{\dagger}_{\mathrm{M}}(\theta)\,|M_+\rangle \\ \hat{U}^{\dagger}_{\mathrm{M}}(\theta)\,|M_-\rangle \end{pmatrix} = \begin{pmatrix} \cos\theta & \sin\theta \\ -\sin\theta & \cos\theta \end{pmatrix} \begin{pmatrix} |M_+\rangle \\ |M_-\rangle \end{pmatrix}, \qquad (17)$$

where θ is the polarization rotation angle from the horizontal plane. The conditioned visibility was measured by varying the object basis while the probe basis was kept fixed. If the rotated probe measurement basis is used, the state (16) can be written

$$\left|\Psi^-\right\rangle = \frac{1}{\sqrt{2}}\{\cos\theta\,[|O_+, M_+(\theta)\rangle - |O_-, M_-(\theta)\rangle] - \sin\theta\,[|O_+, M_-(\theta)\rangle - |O_-, M_+(\theta)\rangle]\}\cdot \qquad (18)$$

After a calculation using equations (13, 14), one finds $D_{\mathrm{m}}(\theta) = |\cos\theta|$ and $V_{\mathrm{c}}(\theta) = |\sin\theta|$. Results of the measurements are shown in Figure 3. Remember that the visibility of this state is zero for any probe measurement basis rotation. The degradation of the conditioned visibility due to the non-perfect mode overlap was taken into account in plotting the solid lines. This was done by multiplying the theoretically predicted conditioned visibility V_{c} by 0.94, which was the maximum experimentally obtained visibility. (For the particular entanglement we chose, the distinguishability relies on energy and momentum conservation, whereas good visibility also requires good mode overlap. The aforementioned group-velocity dispersion associated with short, orthogonally polarized, photon pulses prevented us from getting perfect visibility as can be seen in the figure. Hence, the measured D_{m} goes from very close to unity to zero, whereas V_{c} goes from zero but only reaches 0.94 at its maximum.) The apparent error in the figure is larger than the measurement error of D_{m} and V_{c}, since it is the squares of these quantities, rather than the quantities themselves, that are plotted. We beg the reader to keep this point in mind in the following.

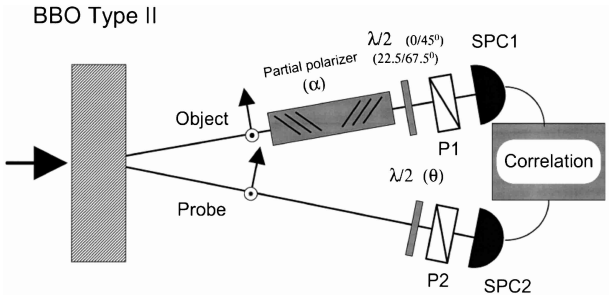

Fig. 4. Experimental setup for non-perfect QND-type measurements of photon polarization.

Note that the effects of quantum erasure are evident in Figure 3. The full information about the "path" taken by the object is available in the state (16) and can be obtained from the probe by an appropriate choice of the probe basis ($\theta = 0°$). However, simply rotating the probe basis will restore full visibility in the object mode (at $\theta = 90°$). Comparing this to the two-slit setup usually considered in discussions about quantum erasure, the probe would interact with the object as the object passes the slits. Depending on the measurement carried out on the probe, we would then either know which slit the object passed through or see an interference pattern on the screen behind the slits.

4.2 Partially entangled states

In order to obtain partially entangled states (case 3 in Sect. 2), a partial polarizer was inserted in the object beam rotated at an angle α to the horizontal plane (see Fig. 4). The partial polarizer consisted of a stack of N glass plates held at the Brewster angle with respect to the stack rotation axis. The amplitude transmittivities of the partial polarizer were $t_{\mathrm{p}} \approx 1$ and $t_{\mathrm{s}} = t$, where t was determined by the number of plates N. (The indices p and s refer to the linear polarization states with respect to the partial polarizer.)

In order to calculate the state after the polarizer, it is convenient to rotate the object and probe bases by the same angle so that the $|O_+\rangle$-state becomes parallel to the

p-plane of the partial polarizer

$$\left|\Psi^{-}\right\rangle = \frac{1}{\sqrt{2}}\left[\left|O_{+}\left(\alpha\right), M_{+}\left(\alpha\right)\right\rangle - \left|O_{-}\left(\alpha\right), M_{-}\left(\alpha\right)\right\rangle\right]. \tag{19}$$

Thus, the state after the partial polarizer is

$$\left|\Psi_{\mathrm{e}}\right\rangle = \frac{1}{\sqrt{1+t^{2}}}\left[\left|O_{+}\left(\alpha\right), M_{+}\left(\alpha\right)\right\rangle - t\left|O_{-}\left(\alpha\right), M_{-}\left(\alpha\right)\right\rangle\right]. \tag{20}$$

A rotation by $-\alpha$ back to the original bases gives

$$\begin{aligned}\left|\Psi_{\mathrm{e}}\right\rangle = {} & a_{1}\left|O_{+}, M_{+}\right\rangle - a_{2}\left|O_{-}, M_{-}\right\rangle \\ & + a_{3}\left(\left|O_{+}, M_{-}\right\rangle - \left|O_{-}, M_{+}\right\rangle\right),\end{aligned} \tag{21}$$

where

$$a_{1} = \frac{t + (1-t)\cos^{2}\alpha}{\sqrt{1+t^{2}}}, \tag{22}$$

$$a_{2} = \frac{t + (1-t)\sin^{2}\alpha}{\sqrt{1+t^{2}}}, \tag{23}$$

$$a_{3} = \frac{(1-t)\sin\alpha\cos\alpha}{\sqrt{1+t^{2}}}. \tag{24}$$

Now, let us find the correlation coefficients with respect to the probe basis rotation. As θ is the angle of the probe measurement basis rotation, the state can be written as

$$\begin{aligned}\left|\Psi_{\mathrm{e}}\right\rangle = {} & b_{1}(\theta)\left|O_{+}, M_{+}\right\rangle - b_{2}(\theta)\left|O_{-}, M_{-}\right\rangle \\ & + b_{3}(\theta)\left|O_{+}, M_{-}\right\rangle + b_{4}(\theta)\left|O_{-}, M_{+}\right\rangle,\end{aligned} \tag{25}$$

where $b_{1}(\theta) = a_{1}\cos\theta - a_{3}\sin\theta$, $b_{2}(\theta) = a_{2}\cos\theta + a_{3}\sin\theta$, $b_{3}(\theta) = a_{3}\cos\theta + a_{1}\sin\theta$, and $b_{4}(\theta) = a_{3}\sin\theta + a_{2}\cos\theta$. The photocount coincidence probabilities become

$$P_{++} = \left|\left\langle O_{+}, M_{+}\left(\theta\right)\left|\Psi_{\mathrm{e}}\right\rangle\right|^{2} = \left|b_{1}(\theta)\right|^{2}, \tag{26}$$

$$P_{--} = \left|\left\langle O_{-}, M_{-}\left(\theta\right)\left|\Psi_{\mathrm{e}}\right\rangle\right|^{2} = \left|b_{2}(\theta)\right|^{2}, \tag{27}$$

$$P_{+-} = \left|\left\langle O_{+}, M_{-}\left(\theta\right)\left|\Psi_{\mathrm{e}}\right\rangle\right|^{2} = \left|b_{3}(\theta)\right|^{2}, \tag{28}$$

$$P_{-+} = \left|\left\langle O_{-}, M_{+}\left(\theta\right)\left|\Psi_{\mathrm{e}}\right\rangle\right|^{2} = \left|b_{4}(\theta)\right|^{2}. \tag{29}$$

Let θ_{0} denote the probe measurement angle defined by $b_{3}(\theta_{0}) = 0$ (for a pure state such an angle always exists). The relation between the states (8) and (25) is then given by

$$w_{+} = \left|b_{1}(\theta)\right|^{2} + \left|b_{3}(\theta)\right|^{2} = \left|b_{1}\left(\theta_{0}\right)\right|^{2} \tag{30}$$

and

$$c = \sqrt{\frac{\left|b_{4}\left(\theta_{0}\right)\right|^{2}}{\left|b_{2}\left(\theta_{0}\right)\right|^{2} + \left|b_{4}\left(\theta_{0}\right)\right|^{2}}} = \sqrt{\frac{\left|b_{4}(\theta_{0})\right|^{2}}{1 - \left|b_{1}(\theta_{0})\right|^{2}}}. \tag{31}$$

Knowing the correlation probabilities it is possible to derive the quantities associated with the "path"

$$\begin{aligned}P &= \left|w_{+} - w_{-}\right| \\ &= \left|\left|b_{1}(\theta)\right|^{2} + \left|b_{4}(\theta)\right|^{2} - \left|b_{2}(\theta)\right|^{2} - \left|b_{3}(\theta)\right|^{2}\right|\end{aligned} \tag{32}$$

and

$$D_{\mathrm{m}}(\theta) = \left|\left|b_{1}(\theta)\right|^{2} - \left|b_{3}(\theta)\right|^{2}\right| + \left|\left|b_{4}(\theta)\right|^{2} - \left|b_{2}(\theta)\right|^{2}\right|. \tag{33}$$

Conditioned visibility can be measured in the same way, if we change the object detector basis from 0/90° to 45/135°. In the new basis, the coincidence probabilities are

$$P_{45++} = \frac{\left|b_{1}(\theta) + b_{4}(\theta)\right|^{2}}{2}, \tag{34}$$

$$P_{45--} = \frac{\left|b_{2}(\theta) + b_{3}(\theta)\right|^{2}}{2}, \tag{35}$$

$$P_{45+-} = \frac{\left|b_{3}(\theta) - b_{2}(\theta)\right|^{2}}{2}, \tag{36}$$

$$P_{45-+} = \frac{\left|b_{4}(\theta) - b_{1}(\theta)\right|^{2}}{2}, \tag{37}$$

which makes it possible to calculate the quantities associated with relative-phase measurements

$$V = \left|P_{45++}(\theta) - P_{45-+}(\theta) + P_{45+-}(\theta) - P_{45--}(\theta)\right| \tag{38}$$

and

$$V_{\mathrm{c}}(\theta) = \left|P_{45++}(\theta) - P_{45-+}(\theta)\right| + \left|P_{45+-}(\theta) - P_{45--}(\theta)\right|. \tag{39}$$

We measured the distinguishability and the conditioned visibility using eight different combinations of partial polarizer rotation angles and number of plates. Here we present only two of the combinations, but all the measurements were in good agreement with theory.

4.2.1 Low a priori "path" information

The measured and calculated data for a home-made, 10-plate, partial polarizer rotated by 43 degrees with respect to the horizontal plane are shown in Figure 5. The 10-plate partial polarizer corresponds to $t = 0.200$. Using equations (21, 7, 9, 10, 11), we can compute the relevant parameters of the state to be $c = 0.716$, $P = 0.065$, $V = 0.925$, and $D = 0.381$, while a direct measurement gives $P = 0.070$, $V = 0.940$, and $D = 0.367$, *via* equations (32, 33, 38). (D is the maximum of $D_{\mathrm{m}}(\theta)$, while V is the minimum of $V_{\mathrm{c}}(\theta)$.) The state differs from the previous one in that although the predictability is almost zero, the distinguishability is nowhere near unity. That is, the object and the probe are only weakly entangled. The results for the D_{m} and V_{c} measurements are shown in Figure 6. One should note specifically that as predicted D_{m} is bound from below by P, and from above by D. In the same manner, we see that V_{c} is bound from below by V, and from above by $(1 - P^{2})^{1/2}$.

It should be noted that the primary data, Figure 5, agrees better with theory than the secondary data, Figure 6. We suspect that the origin of this effect can be traced to our home-made partial polarizer. The partial polarizer glass plates were not mounted perfectly in parallel.

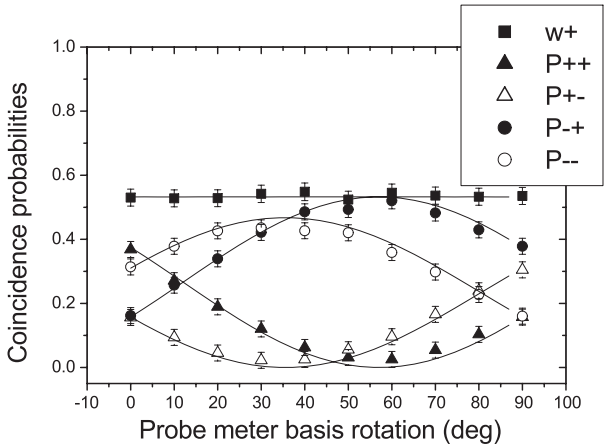

Fig. 5. Coincidence probabilities versus probe meter basis rotation after a 10-plate partial polarizer, rotated by $\alpha = 43$ degrees with respect to the horizontal plane, was inserted in the object beam.

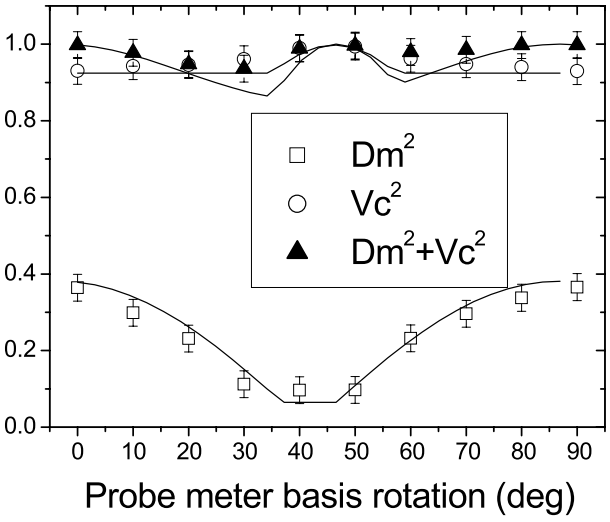

Fig. 6. Results for measured distinguishability and conditioned visibility versus probe meter basis rotation for the case of low *a priori* "path" information.

In an independent measurement, we recorded the transmission of the polarized laser light (before the frequency doubling) through the partial polarizer as a function of the rotation angle α. The transmission curves should be displaced cosine curves, which was not quite the case for our polarizer. However, since we did not possess a goniometer, it was hard to confirm that the suspected imperfection was indeed the cause, so we have opted to publish the uncorrected data.

We can also note that when the state is not perfectly entangled, $D_{\rm m}^2 + V_{\rm c}^2$ is not a conserved quantity although the state is pure, confirming the predictions in [12]. The reason is that the observable corresponding to $V_{\rm c}$ in this case is not strictly complementary to the observable corresponding to $D_{\rm m}$. Therefore, the distinguishability measurement and the visibility measurement do not strictly probe complementary information about the state. However, the sum $D_{\rm m}^2 + V_{\rm c}^2$ saturates the bound (12) when $D_{\rm m} = D$, in accordance with the predictions of [12]. The sharp "corners" in the theoretical curves signify those rotation angles where the maximum likelihood strategy dictates a change in how the probe measurement outcomes should be used for the "path" estimation.

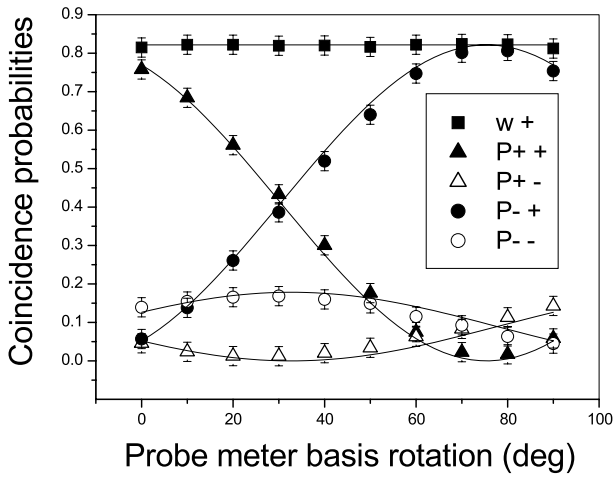

Fig. 7. Coincidence probabilities versus probe meter basis rotation after a 7-plate partial polarizer, rotated by $\alpha = 21$ degrees with respect to the horizontal plane, was inserted in the object beam.

4.2.2 High a priori "path" information

The next example of a complementarity measurement is shown in Figures 7 and 8. In this measurement, a 7-plate glass stack was used as a partial polarizer and the angle of rotation was adjusted to 21°. This corresponds to amplitude transmittivity $t = 0.324$. From these data we can calculate that $c = 0.828$, $P = 0.643$, $V = 0.563$, and $D = 0.839$, which are close to the directly measured experimental values $P = 0.639$, $V = 0.550$, and $D = 0.839$. This state is characterized by its large predictability, in contrast to the previously treated states. Since D must be larger than, or equal to, P, it means that the distinguishability is also high.

In Figure 8, an even more peculiar shape of the function $D_{\rm m}^2 + V_{\rm c}^2$ is seen. Since the predictability is large, there is little information to be had from the probe. We see that for most probe measurement bases the measured distinguishability cannot be improved beyond the *a priori* predictability. Only within a small interval of probe measurement rotations will the information encoded in the state of the probe improve the measured distinguishability, rendering it (at best) equal to D. Similarly, for most rotations, the conditioned visibility does not exceed the visibility V. For the meter basis rotations between about 10 and 30 degrees (in theory) or between 10 and 20 degrees (in the experiment), the measured distinguishability and the conditioned visibility attain their respective minimum values simultaneously. Here, the state is prepared in such a way that the "proper" complementary

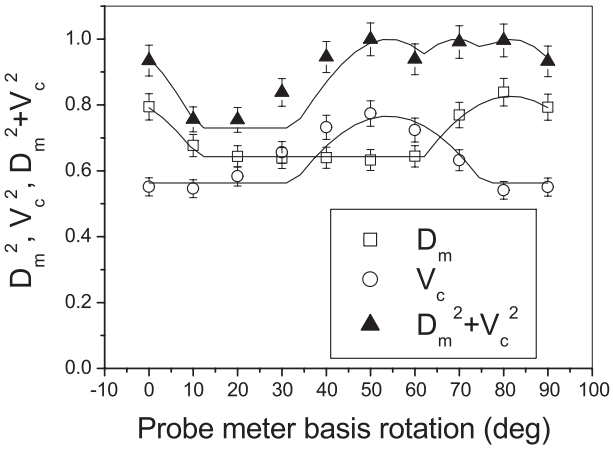

Fig. 8. Results for measured distinguishability and conditioned visibility versus probe meter basis rotation for the case of high *a priori* "path" information.

observable (as defined in [13]) is complementary both to the "path" observable and the conditioned visibility observable. This is a manifestation of the fact that any Hilbert space of dimension two allows three mutually complementary observables.

5 Summary

The complementarity relation quantitatively derived by Englert [11] between "path" information and "path" interference visibility was tested under a wide range of experimental situations. Using a partial polarizer, we were able to generate states with different *a priori* "path" information and different degrees of entanglement. The experiment was designed to, as close as possible, to be an implementation of the theory in [11,12]. This is in contrast to a recent experiment by Schwindt *et al.* [35], where complementarity is tested without employing entanglement and with a larger object Hilbert space than the two-dimensional space prescribed by the theory in [11]. The latter experiment can be analyzed and fully understood in terms of classical physics, whereas the experiment above and, *e.g.*, the experiments reported in [29–32] employ entangled states and hence quantum nonlocality. By changing the measurement basis of the probe (a local operation) and by using conditioned measurements, the experiments gave us the possibility to verify the complementarity relations encompassing quantum erasure [12]. For non-ideal ($P > 0$, $D < 1$) but pure composite states, such a test yields rather surprisingly, only piecewise differentiable curves, reflecting the nonlinear maximum likelihood estimation strategy underlying the theory. Our experimental results were in good agreement with the theoretical predictions.

This work was supported by grants from the Swedish Technical Science Research Council, the Swedish Natural Science Research Council, the Royal Swedish Academy of Sciences, and by INTAS through Grant 167/96.

References

1. W. Heisenberg, Z. Phys. **43**, 172 (1927); H.P. Robertson, Phys. Rev. **35**, 667A (1930); **46**, 7941 (1934); E. Schrödinger, Proc. Prussian Acad. Sci. Phys. Math. Sec. **XIX**, 296 (1930).
2. N. Bohr, Nature **121**, 580 (1928).
3. W.K. Wootters, W.H. Zurek, Phys. Rev. D **19**, 473 (1979).
4. D.M. Greenberger, A. Yasin, Phys. Lett. A **128**, 391 (1988).
5. L. Mandel, Opt. Lett. **16**, 1882 (1991).
6. M.O. Scully, B.-G. Englert, H. Walther, Nature **351**, 111 (1991).
7. M.G. Raymer, S. Yang, J. Mod. Opt. **39**, 1221 (1992).
8. R. Bhandari, Phys. Rev. Lett. **69**, 3720 (1992).
9. S.M. Tan, D.F. Walls, Phys. Rev. A **47**, 4663 (1993).
10. G. Jaeger, A. Shimony, L. Vaidman, Phys. Rev. A **51**, 54 (1995).
11. B.-G. Englert, Phys. Rev. Lett. **77**, 2154 (1996).
12. G. Björk, A. Karlsson, Phys. Rev. A **58**, 3477 (1998).
13. G. Björk *et al.*, Phys. Rev. A **60**, 1874 (1999).
14. E.P. Storey, S.M. Tan, M.J. Collet, D.F. Walls, Nature **367**, 626 (1994).
15. B.-G. Englert, M.O. Scully, H. Walther, Nature **375**, 367 (1995); E.P. Storey, S.M. Tan, M.J. Collet, D.F. Walls, *ibid.* **375**, 368 (1995).
16. H.M. Wiseman, F.E. Harrison, Nature **377**, 584 (1995); H.M. Wiseman *et al.*, Phys. Rev. A **56**, 55 (1997).
17. A. Luis, L.L. Sánchez-Soto, Phys. Rev. Lett. **81**, 4031 (1998).
18. E. Arthurs, J.L. Kelly Jr, Bell Syst. Tech. J. **44**, 725 (1965).
19. E. Arthurs, M.S. Goodman, Phys. Rev. Lett. **60**, 2447 (1988).
20. C.Y. She, H. Heffner, Phys. Rev. **152**, 1103 (1966).
21. S. Stenholm, Ann. Phys. (N.Y.) **218**, 233 (1992).
22. H. Martens, W.M. de Muynck, J. Phys. A **25**, 4887 (1992).
23. D.M. Appleby, Int. J. Theor. Phys. **37**, 1491 (1998); J. Phys. A **31**, 6419 (1998).
24. M.O. Scully, K. Drühl, Phys. Rev. A **25**, 2208 (1982).
25. P.G. Kwiat, A.M. Steinberg, R. Chiao, Phys. Rev. A **49**, 61 (1994).
26. Z.Y. Ou *et al.*, Phys. Rev. A **41**, 566 (1990); Z.Y. Ou, Phys. Lett. A **226**, 323 (1997).
27. X.Y. Zou, L.J. Wang, L. Mandel, Phys. Rev. Lett. **67**, 318 (1991); A.G. Zajonc, L.J. Wang, X.Y. Zou, L. Mandel, Nature **353**, 597 (1991).
28. P.G. Kwiat, A.M. Steinberg, R. Chiao, Phys. Rev. A **45**, 7729 (1992).
29. T.J. Herzog, P.G. Kwiat, H. Weinfurter, A. Zeilinger, Phys. Rev. Lett. **75**, 3034 (1995).
30. T.B. Pittman *et al.*, Phys. Rev. Lett. **77**, 1917 (1996).
31. S. Dürr, T. Nonn, G. Rempe, Phys. Rev. Lett. **81**, 5705 (1998).
32. Y.-H. Kim, R. Yu, S.P. Kulik, Y.H. Shih, M.O. Scully, Phys. Rev. Lett. **84**, 1 (2000).
33. T. Tsegaye *et al.*, Phys. Rev. A **62**, 032106 (2000).
34. P. Bertet *et al.*, Nature **411**, 166 (2001).
35. P.D.D. Schwindt, P.G. Kwiat, B.-G. Englert, Phys. Rev. A **60**, 4285 (1999).
36. J.R. Klauder, E.C.G. Sudarshan, *Fundamentals of quantum optics* (Benjamin, New York, 1968).
37. P.G. Kwiat *et al.*, Phys. Rev. Lett. **75**, 4337 (1995).